

Paper

Comparing the topology optimization results of the stiffest structure using two types of topological derivatives

Takahiko KURAHASHI¹, Manaya NAKAZAWA², Masayuki KISHIDA^{3,4},

Kousuke SHIMIZU⁵ and Tetsuro IYAMA⁶

¹Department of Mechanical Engineering, Institute of GIGAKU, Nagaoka University of Technology

²Mechanical Engineering, Bachelor's Program, School of Engineering, Nagaoka University of Technology
(Current affiliation : ADTEC Engineering Co.,Ltd.)

³Department of Mechanical Engineering, National Institute of Technology, Gifu College

⁴Science of Technology Innovation, 5-year Integrated Doctoral Program, Graduate School of Engineering,
Nagaoka University of Technology

⁵Mechanical Engineering, Master's Program, Graduate School of Engineering, Nagaoka University of Technology

⁶Department of Mechanical Engineering, National Institute of Technology, Nagaoka College

This study examined the effect of varying the approach to obtain the topological derivative and presents the numerical results of level set-based topology optimization for a maximally stiff structure problem. To perform a topology optimization analysis, the performance function was first defined by the strain energy of the structure. The problem was to determine the optimal topology to minimize the performance function under constraint conditions, that is, the governing equation and boundary condition. The adjoint variable method was introduced to address the minimization problem of the performance function under constraint conditions. The optimal topology of the structure was obtained by updating the level-set function, which was achieved by solving the reaction-diffusion equation. The reaction term of the reaction-diffusion equation was expressed by the topological derivative, that is, the gradient of the performance function extended by the adjoint variable and the governing equation with respect to the level-set function. In this study, we varied the method to obtain the topological derivative in level-set-based topology optimization and performed numerical experiments. The finite element method was applied to solve the structural deformation problem.

Key Words: *Level-set-based topology optimization, Maximally stiff structure, Adjoint variable method, Topological derivative, Finite element method*

1. Introduction

Since three-dimensional (3D) printers have gained prevalence, topology optimization analysis has become a focus of attention. Recently, it has been reported that the results of topology optimization

resemble the tissue structure of the bones of living organisms¹⁾. The present study focuses on level-set-based topology optimization, that is, a solution method alongside density-based topology optimization. In some topological optimization problems, the induced topological derivative renders

Comparing the topology optimization results of the stiffest structure using two types of topological derivatives

it difficult to compute the optimal topology²⁾. The topological derivative is specified by the gradient of the objective function with respect to the level-set function, but the convergence rate of the objective function and the accuracy of the optimal solution depends on the gradient, that is, the search direction, such as the relationship between gradient- and Newton-based methods. Therefore, numerical experiments of topology optimization are conducted in this study to maximize stiffness by varying the topological derivative.

2. Derivation of stationary condition of extended performance function

The equivalent, stress–strain relation, and strain–displacement relation equations are expressed as Eqs. (1)–(3), respectively. These equations are written using the summation convention.

$$\sigma_{ij,j} = 0 \quad (1)$$

$$\sigma_{ij} = D_{ijkl}\epsilon_{kl} \quad (2)$$

$$\epsilon_{ij} = \frac{1}{2}(u_{i,j} + u_{j,i}) \quad (3)$$

Here, σ_{ij} , ϵ_{ij} , D_{ijkl} and u_i indicate components of stress and strain tensors, the elasticity coefficient tensor and the displacement components, respectively. If the finite element Galerkin procedure is applied to discretize Eqs. (1)–(3), then the finite element equation shown in Eq. (4) can be derived³⁾. \mathbf{u}_e and \mathbf{f}_e denote displacement and external force vectors, respectively. \mathbf{K}_e represents the stiffness matrix and is calculated using Eq. (5). \mathbf{B}_e and \mathbf{D}_e indicate the matrix B and the elasticity coefficient matrix, respectively.

$$\mathbf{K}_e \mathbf{u}_e = \mathbf{f}_e \quad (4)$$

$$\mathbf{K}_e = \int_{\Omega_e} \mathbf{B}_e^T \mathbf{D}_e \mathbf{B}_e d\Omega \quad (5)$$

Superposing Eq. (4) for all elements, the finite element equation for the entire domain is obtained as shown in Eq. (6). The boundary condition is defined by Eq. (7). Γ_1 and Γ_2 indicate the Dirichlet and Neumann boundaries, respectively, and the hat

symbol indicates the specified value.

$$\mathbf{K}\mathbf{u} = \mathbf{f} \quad (6)$$

$$\begin{cases} \mathbf{u} = \hat{\mathbf{u}} & \text{on } \Gamma_1 \\ \mathbf{f} = \hat{\mathbf{f}} & \text{on } \Gamma_2 \end{cases} \quad (7)$$

Here, we consider the maximally stiff structural problem. The maximally stiff structure is a structure that minimizes strain energy. Therefore, the performance function is defined by the strain energy, as shown in Eq. (8). Substituting Eq. (6) into the external force vector \mathbf{f} yields Eq. (8), which is represented by the stiffness matrix \mathbf{K} and displacement \mathbf{u} .

$$J = \frac{1}{2} \mathbf{u}^T \mathbf{f} = \frac{1}{2} \mathbf{u}^T \mathbf{K} \mathbf{u} \quad (8)$$

The problem is to determine the optimal topology to minimize the performance function J . To obtain the displacement vector, the finite element equation shown in Eq. (6) must be solved. Therefore, this is a minimization problem with a constraint condition, as shown in Eq. (6). Using the adjoint variable method, the performance function is extended by the adjoint variable vector $\boldsymbol{\lambda}$ and finite element equation, Eq. (6), and the extended performance function is expressed as shown in Eq. (9). Eq. (9) is referred to as the Lagrange function. Here, the stiffness matrix \mathbf{K} is expressed by the characteristic function χ , and the characteristic function χ is the function of the level-set function ϕ . If the level-set function ϕ is positive, then the element is in the material domain. If the level-set function ϕ is negative, then the element is in the void domain. If the level-set function ϕ is zero, then the boundary is between the material and void domains. The characteristic function χ is 1 when the element is in the material domain, and 0 when the element is in the void domain. The stiffness matrix \mathbf{K} is employed when χ is 1. The stiffness matrix \mathbf{K} is expressed by a zero matrix when χ is 0.

$$J^* = \frac{1}{2} (\mathbf{u}^T \mathbf{K}(\chi(\phi)) \mathbf{u} + \boldsymbol{\lambda}^T (\mathbf{K}(\chi(\phi)) \mathbf{u} - \mathbf{f})) \quad (9)$$

To control the complexity of the structure, a regularization term is generally included in the

Lagrange function in level-set-based topology optimization. To derive the discretized regularization term, we introduce the steady-state diffusion equation shown in Eq. (10). τ and ϕ represent the regularization parameter and level-set function, respectively. The finite element Galerkin procedure is applied to Eq. (10), which results in Eq. (11). \mathbf{H} and \mathbf{q} indicate the diffusion matrix and heat-flux vector, respectively. The boundary conditions for Eq. (11) are shown in Eq. (12).

$$\tau\phi_{,ii} = 0 \quad (10)$$

$$\tau\mathbf{H}\phi = \mathbf{q} \quad (11)$$

$$\begin{cases} \phi = \hat{\phi} & \text{on } \Gamma_1 \\ \mathbf{q} = \hat{\mathbf{q}} & \text{on } \Gamma_2 \end{cases} \quad (12)$$

The regularization term, expressed in Eq. (11) is added to the Lagrange function, J^* . In addition, a volume constraint condition is added to the Lagrange function J^* . Finally, the modified Lagrange function K is defined as shown in Eq. (13). Λ , v_e , and V_{max} indicate the adjoint variable, element volume, and target volume, respectively. χ_e represents the characteristic function. The value of χ_e is 1 when the element is in the material domain. However the value of χ_e is 0 when the element is in a defect domain, that is, a void domain. mx refers to the number of elements.

$$J^{**} = J^* + \frac{1}{2}\tau\phi^T\mathbf{H}\phi + \Lambda(\sum_{e=1}^{mx}\chi_e(\phi)v_e - V_{max}) \quad (13)$$

To obtain the stationary condition of the modified Lagrange function J^{**} , the first variation of the modified Lagrange function J^{**} is calculated. From the gradient of the modified Lagrange function J^{**} with respect to the adjoint variable vector λ , the finite element equation for elastic deformation is obtained (see Eq. (14)). From the gradient of the modified Lagrange function J^{**} with respect to the displacement vector \mathbf{u} , the adjoint equation is obtained (see Eq.(15)). Eq. (16) can be obtained from Eq. (14), and Eq. (17) can be obtained from Eq. (15). Comparing Eqs. (16) and (17), the relation equation between the displacement vector and adjoint variable vector is derived as shown in Eq. (18). This relationship is referred to as the self-adjoint

relationship.

$$\frac{\partial J^{**}}{\partial \lambda} = \mathbf{K}(\chi(\phi))\mathbf{u} - \mathbf{f} = \mathbf{0} \quad (14)$$

$$\begin{aligned} \frac{\partial J^{**}}{\partial \mathbf{u}} &= \mathbf{K}(\chi(\phi))\mathbf{u} + \lambda^T\mathbf{K}(\chi(\phi)) \\ &= \mathbf{f} + \mathbf{K}^T(\chi(\phi))\lambda = \mathbf{0} \end{aligned} \quad (15)$$

$$\mathbf{K}(\chi(\phi))\mathbf{u} = \mathbf{f} \quad (16)$$

$$\mathbf{K}^T(\chi(\phi))\lambda = -\mathbf{f} \quad (17)$$

$$\mathbf{u} = -\lambda \quad (18)$$

In addition, the level-set function vector ϕ is updated by the gradient of the modified Lagrange function J^{**} with respect to the level-set function vector ϕ . The update of the level-set function is performed using the Allen–Cahn equation, which is discretized by the finite element method (see Eq. (19)). Here, \mathbf{M}_e indicates the mass matrix. If $\frac{\partial J^{**}}{\partial \phi}$ is calculated, then Eq. (19) can be represented by Eq. (20). Eq. (20) can be expressed as Eq. (21), which shows the reaction-diffusion equation. Parameter C is the normalization parameter and is expressed as $C = \frac{mx}{\sum_{e=1}^{mx}|\frac{\partial J^*}{\partial \phi_e}|}$. This parameter is adjusted for each iteration step.

$$\mathbf{M}_e \frac{\partial \phi_e}{\partial t} = -\alpha \frac{\partial J^{**}}{\partial \phi_e} \quad (19)$$

$$\mathbf{M}_e \frac{\partial \phi_e}{\partial t} = -\alpha \left(C \frac{\partial J^*}{\partial \phi_e} + \tau\mathbf{H}_e\phi_e + \Lambda \right) \quad (20)$$

$$\mathbf{M}_e \frac{\partial \phi_e}{\partial t} + \alpha\tau\mathbf{H}_e\phi_e = -\left(C \frac{\partial J^*}{\partial \phi_e} + \Lambda \right) \quad (21)$$

According to a previous study⁴⁾, $\frac{\partial J^*}{\partial \phi_e}$ is calculated using Eq. (22), and \mathbf{K}'_e is represented by Eq. (23). In matrix \mathbf{K}'_e , matrix \mathbf{A}_e in the two-dimensional plane-stress state is expressed as Eq. (24). Here, A_1 and A_2 are calculated using Eq. (25).

$$\frac{\partial J^*}{\partial \phi_e} = \lambda_e^T \mathbf{K}'_e \mathbf{u}_e = -\mathbf{u}_e^T \mathbf{K}'_e \mathbf{u}_e \quad (22)$$

$$\mathbf{K}'_e = \int_{\Omega_e} \mathbf{B}_e^T \mathbf{A}_e \mathbf{B}_e d\Omega \quad (23)$$

$$\mathbf{A}_e = \begin{bmatrix} A_1 + 2A_2 & A_1 & 0 \\ A_1 & A_1 + 2A_2 & 0 \\ 0 & 0 & A_2 \end{bmatrix} \quad (24)$$

Comparing the topology optimization results of the stiffest structure using two types of topological derivatives

$$\begin{cases} A_1 = -\frac{3(1-\nu)(1-14\nu+15\nu^2)}{2(1+\nu)(7-5\nu)(1-2\nu^2)}E \\ A_2 = -\frac{15(1-\nu)}{2(1+\nu)(7-5\nu)}E \end{cases} \quad (25)$$

$\frac{\partial J^*}{\partial \phi_e}$ is the topological derivative and is derived for each topological-optimization problem. Matrix \mathbf{K}'_e , that is, Eq. (23), is similar to stiffness matrix \mathbf{K}_e shown in Eq. (5). Therefore, in this study, numerical experiments were performed by changing matrix \mathbf{K}'_e to stiffness matrix \mathbf{K}_e when computing $\frac{\partial J^*}{\partial \phi_e}$. An image diagram of the flow of the level-set-based topology optimization is shown in Fig. 1 (see reference⁵ for details.).

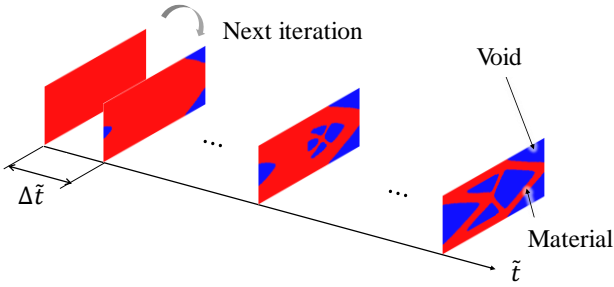


Fig.1 Image diagram of the flow of level-set-based topology optimization.

3. Numerical experiments

Numerical experiments for the level-set-based topology optimization analysis of the maximally stiff structure problem were conducted by varying the method to obtain the topological derivative. The computational model is shown in Fig. 2, and the computational conditions are listed in Table 1. Deformation analysis was performed under a two-dimensional plane-stress state.

The computational model is illustrated in Fig. 2. The aim of this study was to determine the optimal topology to minimize the strain energy of the structure. In this study, the numerical results were compared by changing the method for providing the topological derivative. The elasticity coefficient

matrix \mathbf{D}_e was employed instead of matrix \mathbf{A}_e in the calculation of the topological derivative⁶). Therefore, in the setting of matrix \mathbf{K}'_e , the matrix shown in Eq. (23) was employed in case 1, the elasticity coefficient matrix \mathbf{D}_e was applied to calculate the matrix \mathbf{K}'_e instead of matrix \mathbf{A}_e in case 2, and the numerical results were compared.

The numerical results are as follows. Figs. 3 and 4 show the variations in the level-set and characteristic functions, respectively. The optimal topology is expressed using a characteristic function. If the level-set function is positive, then the characteristic function is 1 and the element represents the material domain. However, if the level-set function is negative, then the characteristic function is zero and the element represents the void domain. Based on a comparison between cases 1 and 2, although a slightly different shape is obtained in the midst of the iterative computation, a similar shape is obtained in the final iteration.

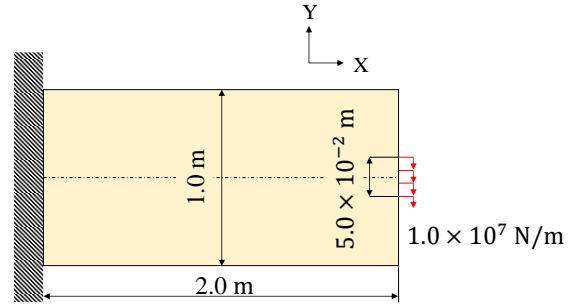


Fig.2 Computational model

Table 1 Computational conditions

Number of nodes / elements	12800 / 13041
Mesh size Δx [m]	1.25×10^{-2}
Young's modulus E [GPa]	206
Poisson's ratio ν	0.3
Virtual time $\Delta \tilde{t}$	0.7
Volume reduction rate [%]	55
Number of steps for volume reduction n_{vol}	100
Design domain for topology optimization [m ²]	2.0×1.0
Convergence criterion ϵ_{opt}	1.0×10^{-6}
Regularization parameter τ	3.0×10^{-4}

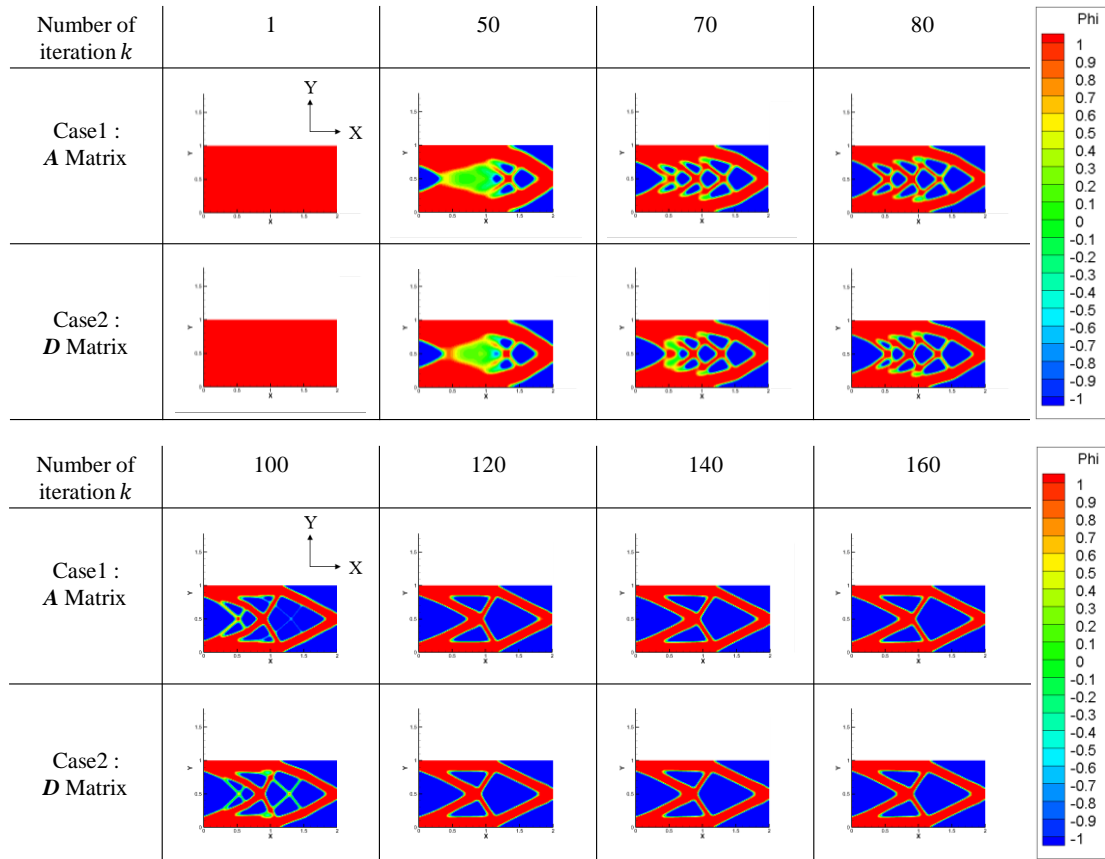


Fig. 3 Variation in level-set function.

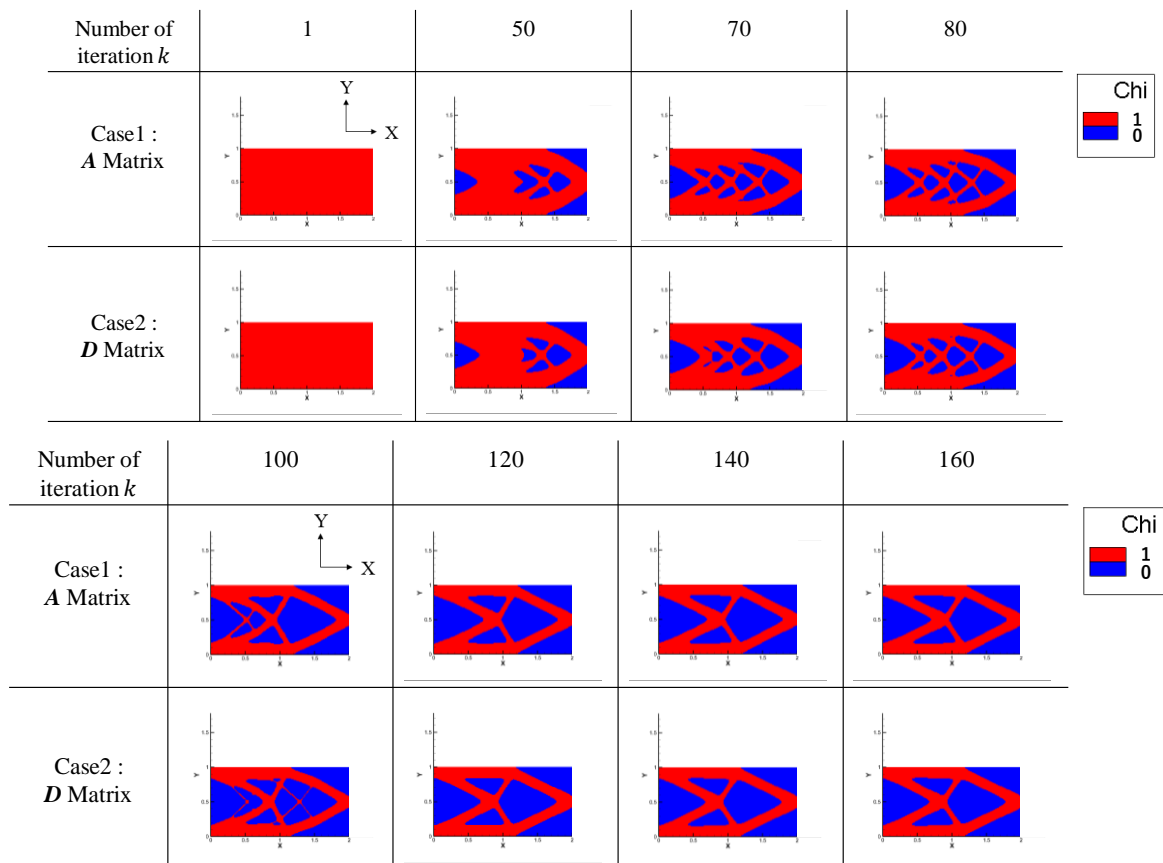


Fig. 4 Variation in characteristic function.

4. Conclusions

In this study, numerical results were obtained by changing the method for obtaining the topological derivative in level-set-based topology optimization. The maximally stiff structural problem was solved for the optimization problem, and the cantilever beam model was introduced as a numerical example. The results showed that even if matrix \mathbf{A}_e in the topological derivative can be replaced by an elasticity coefficient matrix \mathbf{D}_e , an appropriate optimized topology can be obtained.

Additionally, we developed a new updated equation for the design variable⁷⁾. In the future, we aim to apply the new update equation to the present method and investigate the effect of the convergence rate of the performance function.

Acknowledgments: The computations were mainly performed using computer facilities at Kyushu University's Research Institute for Information Technology. We wish to thank the staff at Kyushu University's Research Institute for Information Technology. We would like to thank Editage (www.editage.com) for English language editing.

References

- 1) N. Aage, E. Andreassen, B.S. Lazarov and O. Sigmund: *Giga-voxel computational morphogenesis for structural design*, Nature, Vol. 550, pp.84-86, 2017.
- 2) T. Nakazono and H. Yoshikawa: *An identification of defects using topological derivatives for nondestructive evaluation of elastic materials with laser interferometry data*, Transactions of the Japan Society for Computational Methods in Engineering, Vol. 22. No.1, pp.171-177, 2022. (In Japanese.)
- 3) M. Kawahara : *Finite element methods in incompressible, adiabatic, and compressible flows*, Springer, 2016.
- 4) M. Otomori, T. Yamada, K. Izui and S. Nishiwaki: *Matlab code for a level set-based topology optimization method using a reaction diffusion equation*, Structural and Multidisciplinary Optimization, Vol.51, No.5, pp.1159-1172, 2014.
- 5) S. Nishiwaki, K. Izui and N. Kikuchi: *Topology optimization*, Maruzen Publishing Co.,Ltd., 2013. (In Japanese.)
- 6) T. Yamada, K. Izui, S. Nishiwaki and A. Takezawa : *A*

topology optimization method based on the level set method incorporating a fictitious interface energy, Computer Methods in Applied Mechanics and Engineering, 199, pp.2876–2891, 2010.

- 7) H. Arata, M. Kishida and T. Kurahashi : *Texture shape optimization analysis using a new acceleration gradient method based on the Taylor expansion and conjugate direction*, Journal of Fluid Science and Technology, Vol.17, No.4, pp.1-12, 2022.

(Received July 19, 2023)